SPE 134293

A New Cost Effective Well Testing Methodology for Tight Gas Reservoirs

Antoine Jacques - Total, SPE, Benoît Brouard - Brouard Consulting, SPE, Pierre Bérest - Ecole Polytechnique (Paris), Jean-Luc Boutaud de la Combe, SPE, Total

This paper was prepared for presentation at the SPE Annual Technical Conference and Exhibition held in Florence, Italy, 19–22 September 2010.

Abstract

Obtaining formation characteristics in a tight-gas environment is highly challenging: formation tester tools run during open-hole logging are often unsuccessful, and conventional well tests are not appropriate as no gas flow is commonly observed before hydraulic fracturing. This paper presents a new well testing methodology adapted from techniques used in the salt industry and successfully applied to Tight Gas Reservoirs, using only wellhead pressure gauges and surface flow meters without downhole tools. It delivers an injectivity index profile along the open hole, allowing better identification of the zones with the best potential and optimization of the hydraulic fracturing strategy. The test typically consists, after having run a tubing string, in continuously displacing the annulus mud by a heavier and less viscous fluid such as brine. During the test, the mud/brine interface rises up along the borehole as a result of pumping brine down the tubing at constant pressure and circulating out mud from the annulus. As viscosities and densities are contrasted, brine and mud injection rates in a given layer are also expected to be contrasted. The differences between brine and mud flow rates provide a continuous injectivity indicator along the wellbore. A different procedure, involving stationary step-by-step measurements, can also be performed. The fluid interface is displaced to a predetermined depth, at which step the entire wellbore is pressurized and a fall-off resulting from fluid leak-off across the open hole is recorded and analyzed to derive a layer productivity index.
To date, three well tests have been carried out in various types of wells, showing good correlations with conventional logs. To go a step further than a qualitative tool, a deconvolution of the time-dependent and interface-depth-dependent permeation flows is necessary. An inversion process accounting for the injection history in the various layers is being developed with the objective of deriving a continuous *kh* and skin profile. This new method still needs to be qualified against conventional *kh* data. In particular, it must be demonstrated that the test provides access to the *kh* of the undamaged zone of the wellbore.

Introduction

Conventional well testing cannot be applied in Tight Gas Reservoirs as initial flow rates from the rock formation in low-permeability zones are too small to be measured. Conversely, after hydraulic fracturing performed to establish commercial production, very long shut-in times are required to reach radial flow. Yet an optimum fracturing strategy, specifically for deep and thick gas reservoirs, is a prerequisite for obtaining commercial success in an unconventional context. Knowledge of the formation's dynamic characteristics along the length of the open hole would be invaluable in such a context.
Other industries than Oil & Gas, operating in a tighter economical environment, have developed low-cost methods to meet their own needs in well testing. In the underground storage industry, interest in understanding the very long-term behavior of deep salt caverns has increased due to growing concern for environmental protection. Specific testing methods have been developed to differentiate between fluid leaks through the cemented casing and fluid seeps through the rock formation occurring in solution-mined cavities **(Figure 1).** One

classic method consists of displacing or circulating a nitrogen fluid column below the casing shoe into the annular space between the central tube and the last cemented casing, and monitoring the displacements of the nitrogen/brine interface by means of wellhead pressures measurements. Upward displacement of the interface is interpreted as a nitrogen leak-off. This testing procedure allows the sealing efficiency of the cemented production casing to be checked without any interference from the phenomena which affect the cavern itself.
The central idea of this technique is to create a clean fluid interface in the well annular space between two non miscible fluids, in order to be able to differentiate fluid leak-offs in two different zones, i.e. the well and the cavern itself. This paper explains how the basic principle of this technique has been adapted and generalized to a hydrocarbon well to derive dynamic information on the entire open hole in a cost-effective manner.

- With this new method, the angle of reservoir testing is changed. We are considering the actual well fluid volume that can leak off into the formation rather than the classical interpretation of radial flow into the formation. Lengthy testing is therefore unnecessary as it is the liquid losses from the well rather than the established radial flow in the reservoir that are interpreted. Wellbore storage is taken into account via modeling of well, formation and fluid compressibilities and is calibrated against measurements during the testing phase. Creating an interface between two contrasting liquids in the open hole, as in the original method, allows fluid losses of the less viscous fluid to be estimated in the part of the open hole exposed to flow injectivity **(Figure 2).** Compared to conventional well testing in injection, the fluid interface acts as a kind of packer, splitting the open hole into two parts. The lower section is open to injection of the less viscous fluid, i.e. brine, while the upper section is almost closed, with a very small injection rate of the more viscous fluid, i.e. drilling mud. However, the very small drilling mud leak-off rate into the formation is taken into account when the test is interpreted.
- Thanks to huge progress in recent years in computation capacity, the test procedure can be generalized and run continuously to log the entire open hole by slowly displacing the mud/brine interface along the borehole. The moving fluid interface is in fact acting as a “moving fluid packer” which, little by little, exposes the open hole to brine injectivity. This combination of well testing and logging requires a deconvolution of the time-dependent and interface-depth-dependent permeation flows. Specific finite element software and inversion algorithms have been developed for the purpose.
- Keeping costs as low as possible is crucial in the unconventional context. Test duration can be kept to a minimum by avoiding a special trip to install a dedicated service string for the test. The production tubing is run with float equipment, just before cementing operations, to test the deep gas well and displace the fluid interface along the open hole. It took 4 hours to record 500 meters of open hole in the continuous phase, i.e. an interface speed of about 2 meters/min. Sensitivity to circulation rate will later be analyzed to define the optimum pumping rate while logging. Circulations rates of up to 4 meters/min were tested in a repeat section, showing similar events. Furthermore, this well test method requires only wellhead pressure gauges and flow meters at the inlet and the outlet of the well; no downhole tool is needed.

Three well tests have been carried out to date in various type of wells, namely a shallow well in a non-reservoir zone (200 mRT), a medium-deep vertical gas well (1800 mRT) and a deep deviated gas well (3900 mRT).Very good qualitative results and excellent matching with open-hole logs were obtained. The ultimate objective of this new method is to derive a continuous permeability and skin profile. A qualification process for achieving that goal through additional tests and calibration against conventional well test data is in progress.

Background Theory

The following is a summary of the basic principles of the testing method, both in continuous mode when the open hole is exposed to brine injection by slowly displacing the mud/brine interface along the borehole and in fall-off mode when stationary pressure steps are recorded.

Let P_{tub}^{wh} and P_{ann}^{wh} be the wellhead pressures in the central tube and in the annular space, respectively; $Q_{ann}^{wh} > 0$ and $Q_{tub}^{wh} > 0$ are the circulation flow rates of the lighter and heavier liquids as measured at the wellhead; $Q_1 > 0$ and $Q_2 > 0$ are the permeation flow rates of the lighter and heavier liquids injected in the rock formation, respectively).

Continuous-mode well test

The test typically consists, after having run a tubing string, of continuously displacing the drilling mud by a heavier and less viscous fluid such as brine. During the test, the mud/brine interface rises up along the borehole as a result of pumping brine down the central tubing and circulating out mud from the annulus. Wellhead tubing pressure is kept constant throughout the test. Only wellhead pressure gauges and surface flowmeters are necessary for test interpretation.

The varying interface location in the open-hole is $h = h(t)$ (**Figure 2**). Mass conservation is written:

$$\begin{cases} \dfrac{d}{dt}\displaystyle\int_0^{H_{cas}+H_d-h} \rho_1(z)\,S_{ann}(z)\,dz = -\rho_1\left(Q_{ann}^{wh}+Q_1\right) \\ \dfrac{d}{dt}\left[\displaystyle\int_0^{H_{cas}+H_d} \rho_2(z)\,S_{tub}(z)\,dz + \int_{H_{cas}+H_d-h}^{H_{cas}+H_d} \rho_2(z)\,S_{ann}(z)\,dz + \right] = \rho_2\left(Q_{tub}^{wh}-Q_2\right) \end{cases} \quad (1)$$

Liquid densities (ρ_1 and ρ_2), central tube and annular cross sections (S_{tub} and S_{ann}) are functions of depth, pressure and temperatures, which are also functions of depth and time. Liquids densities at the wellhead are continuously measured during the test through accurate mass flowmeters. Pressures rates can be computed using the mechanical equilibrium conditions and in particular:

$$\frac{d}{dt}\left[P_{ann}^{wh} + \int_0^{H_{cas}+H_d-h} \rho_1(z)\,g\,dz\right] = \frac{d}{dt}\left[P_{tub}^{wh} + \int_0^{H_{cas}+H_d-h} \rho_2(z)\,g\,dz\right] \quad (2)$$

Temperature variations raise a more difficult problem. When liquid displacements are very slow, their vertical temperature distribution reaches equilibrium with the geothermal temperature distribution. When displacements are faster, heat exchanges between the central tube and the annular space and between the annular space and the rock mass must be accounted for, especially in deep formations. Due to thermal expansion, the volume of fluid coming out of the annulus may be in fact greater than the volume of fluid pumped into the central pipe, although some liquid is injected into the formations.

After some algebra, (1) and (2) lead to a linear relation between, on the one hand, the permeation flow rates injected into the formation (Q_1 and Q_2) and the interface displacement rate ($\dot{h} = dh/dt$) and, on the other hand, the wellhead pressure rates:

$$\begin{bmatrix} Q_1 + Q_{ann}^{wh} \\ Q_2 - Q_{tub}^{wh} \\ (\rho_2 - \rho_1)\,g\dot{h} \end{bmatrix} = [M] \begin{bmatrix} \dot{P}_{tub}^{wh} \\ \dot{P}_{ann}^{wh} \end{bmatrix} \quad (3)$$

Where $[M]$ is a 3×2 matrix whose coefficients (see Appendix) depend on liquids and well compressibility, on well geometry and interface location ("*well coupling*"). These coefficients can be estimated before the tests; however it is useful to calibrate their numerical values through *in situ* compressibility tests, which can easily be performed during the tests. Precise assessment of Q_1 and Q_2 requires that (3), which is a differential equation with respect to $h = h(t)$, be integrated with respect to time.

In this acquisition mode, the heavy liquid is pumped continuously into the central tube ($Q_{tub}^{wh} > 0$) and light liquid outflow ($Q_{ann}^{wh} > 0$) may be choked in such a way that interface displacement rate is kept roughly constant. A pressure regulator must also be used to keep tubing wellhead pressure constant ($\dot{P}_{tub}^{wh} = 0$).

Fall-off mode well test

Stationary measurements ("pulse" tests) can also be run at particular depths selected with the help of open-hole logs in order to define interesting zones or layers (reservoir and non-reservoir). At each step or depth interval, the entire wellbore is pressurized. Fracturing pressure must not be exceeded. The fall off resulting from fluid leak-off across the open hole is monitored with high resolution pressure gauges which are set both at the wellhead and

at the tubing and annulus sides. In this particular configuration, the wellhead is closed ($Q_{ann}^{wh} = Q_{tub}^{wh} = 0$). Well pressure is increased rapidly at the beginning of the test and a fall-off period is observed.

Inversion process

During the test, the liquid flow rates injected in the formation, or Q_1 and Q_2, can be assessed *separately* as a function of time through (3). From logs run during well drilling, a first picture of the rock formation is available: a dozen or so different layers can be identified, and, for each of these layers, porosity, permeability and skin can be at least roughly estimated. From this first set of data, a theoretical response of the formation to pressure changes during the test can be predicted, and liquid flow rates injected into the formation can be computed. These are compared to the as-observed flow rates which, as explained above, were inferred from well head measurements. An optimization process can be engaged. The main unknowns are layer permeabilities and skins. At each step, new values of these properties are selected, according to a modified Nelder-Mead algorithm, and tested. The objective function (for instance, in the case of a "fall-off" test) is the difference between computed and as-observed wellhead pressure histories. A better match is reached progressively. After several hundreds of computations, an acceptable match is found and injectivity profiles are obtained.

Field cases

To date, three well-test logs have been carried out in various types of wells. A first experimental pilot was run in a medium-depth vertical gas well (1800 mRT) to experiment the principle of the method by carrying out a succession of fall-offs along the open hole. A second experimental pilot tested the continuous mode in a shallow well (200 mRT) to prepare a demonstration pilot in a deep, deviated gas well (3900 mRT) using the same test procedures.

First experimental pilot – Medium-depth vertical gas well (1800 mRT) – Fall-off mode

This first pilot test was performed in a complex and challenging reservoir configuration. The casing shoe of this vertical well was set at 1200 mRT and the 600-meter high open hole included a highly permeable water reservoir at the top of the open-hole section and a tight-gas reservoir objective between 1680 and 1800 mRT.
In this first case, the test was carried out by reverse circulation and involved a step-by-step procedure with only pressurization of the wellbore and a subsequent fall off at each step. The heavy liquid in the central tube was a water-based drilling mud and the lighter liquid in the annular space was a brine.

- Brine was pumped in reverse into the annulus and the brine/mud interface moved downward along the open hole; these conditions were not favorable, as the permeable water reservoir was exposed to brine injection throughout the test. Additionally, monitoring of the fluid interface was difficult, as wellbore condition and pumping equipment (pumps and flow meters) were poorly suited to small flow rates. The main difficulties arose from an inadequate brine injection pump, inducing severe pressure pulses and unreliable flow meters, especially where mud outflow measurement was concerned. As a consequence, it was not possible to determine the interface depth in real time during the test and the initial program, which included a detailed investigation of the reservoir section, was not fully completed. Nevertheless, the full test history has been *a posteriori* reconciled and the position of the fluid interface at each fall-off step accurately defined thanks to down-hole pressure gauges installed in the tubing string, which was run specifically for the test.
- The heavy liquid in the central tube was a typical water-based drilling mud and the lighter liquid in the annular space was almost-soft water; their specific gravities were 1.18 and 1.02 respectively. The viscosities of the two liquids were contrasted: 35 cP for the water-based mud and 5 cP for the slightly viscosified brine. A typical test step consisted of pressuring the well by brine injection, after which a pressure fall-off was observed for a period of 30 minutes to one hour **(Figure 3).** Between steps, the interface was displaced by injecting brine down the annular space and circulating mud out from the central tubing. As the liquid viscosities were contrasted, time-dependent and interface-depth-dependent fall-offs were different. Optimization algorithms were used to match well-head pressure during fall-offs (**Figure 4),** allowing back-calculation of the layers' hydraulic properties along the borehole (**Figure 5**).

Inversion computations of the other fall-offs confirmed that the top water-bearing reservoir layer was relatively permeable compared to the other layers and that its average permeability was of the order of 6 to 15 mD. This layer also appeared to show a high skin value, probably due to mud cake or fluid invasion during drilling and possibly also during the actual test.

The layers at the bottom of the open–hole section of this reservoir appeared to be much less permeable. As the permeable reservoir layer was involved in almost all the test steps, accurate back-calculation of the permeability of the tight zone using the current inversion algorithm was not an easy task. However, an estimate of the overall tight reservoir permeability, at about 0.26 mD, was close to conventional estimates, derived from core/log correlations of adjacent wells, but could not be checked against conventional well test data due to inconclusive test interpretation.
At that time, it was decided to drastically improve flow measurements in order to obtain accurate real-time monitoring of interface depth during the test. As it had proved difficult during the test to relate log events to real time data, it was proposed to develop a continuous acquisition mode instead of a fall-off step mode, a change made possible by the huge advances in computation capacity in recent years. This type of acquisition is key to the success of this new methodology, which combines well testing and logging to derive a continuous permeation profile matched against conventional log data. As in conventional PLT, an injection profile is determined first, after which stationary fall-off steps are carried out for further calibration. The well test procedure, especially concerning the unusual reverse circulation via the annulus, also needed to be revisited

Second experimental pilot - Shallow well in a non-reservoir zone (200 mRT) - Continuous mode

In light of the encouraging results and field experience gained during the first pilot test, it was decided to run another test in a deep gas well with an enhanced test monitoring & acquisition system so as to obtain a high-quality data set and to be able to qualify this new testing method in an industrial context. To save rig costs, a pre-test pilot in a shallow, non-reservoir well was planned with the following objectives: run the test in the same configuration as was used for the deep well test, check the measuring devices and the acquisition system, test the continuous fluid circulation mode in addition to the earlier mode based on several injection/ fall-off sequences and compare test results against core & log data in a non-reservoir environment.

- Test operations were conducted in a shallow vertical well with a casing shoe set at 67 mRT in mudstone cap rocks, from 70 to 200 meters deep, overlying a salt layer (the well was drilled for salt production by solution-mining). Data acquisition included coring with a 5¼" core head, which led to approximately 50% recovery of the overall interval. A log suite (GR, Res, Neutron-Density) was acquired after the hole was opened to 6". Well tests were then conducted in the 6" open hole through a centralized 2⅞" tubing string.
- To run the test in the same configuration as in the planned deep well test, the light liquid, supposed to mimic the oil-based drilling mud, was organic colza oil, an environment-friendly liquid. Its specific gravity was 0.92 and its viscosity was approximately 70 cP or so at ambient conditions. The use of this type of oil was a good compromise but its behavior, where filtration limitation is concerned, was obviously very different from that of a typical drilling mud. The heavy liquid was a non-saturated brine with a density of 1.08 and a viscosity of about 1.4 cP.
- The test started once the annulus was full of the viscous colza oil, then, as planned for the deep well test, the well test consisted here of continuously displacing the colza oil by the heavier, less viscous brine. During the test, the brine/colza oil interface moved upward along the borehole as a result of pumping brine down the central tubing at a constant pressure and circulating out colza oil from the annulus.
- All equipment and procedures were successfully tested. Two continuous circulation tests were carried out in the open hole, showing consistent but unexpected results.

Unfortunately, the presence of an unplanned layer more permeable than the underlying shaly levels was detected close to the 6" casing shoe, between 67 mRT and 75 mRT. A review of the well's stratigraphic column with the help of core and log data highlighted the presence of a secondary water-bearing layer. This layer was not covered by the 6" casing which had been set to isolate a sandstone water reservoir, well known in the area. Unfortunately, we were back in the situation experienced in the first pilot, characterized by a highly permeable reservoir at the top of the open hole, which hindered correct interpretation of the properties of the very tight underlying layers (**Figure 6)**. As the fluid loss properties of the colza oil are far less efficient than a conventional drilling mud, which has a cake building effect, the colza oil injection rate in the permeable reservoir was still significant compared to the brine injection rate in tight layers. This configuration was far from the assumption of the theoretical model, in which the injectivity of the more viscous fluid in the open hole is much lower than that of the less viscous fluid.

Nevertheless, though difficult to interpret, the raw data proved to be quite encouraging, as the permeable layer (unknown before the test) was accurately detected during the continuous test; vertical resolution was excellent. Moreover, in spite of the strong influence of the permeable (>100 mD) aquifer layer, vertical differences in the characteristics of the tight (<0.1 mD) shaly layer can be identified from the raw injectivity

profile and correlated with log data **(Figure 7**). A refined analysis of test data will be undertaken once the core measurements & log data interpretation are fully completed. Further development of the theory to suit this particular case will be considered if needed. It was felt that a standard drilling mud would have been much more efficient than colza oil to build a mud cake on the permeable reservoir and limit fluid filtration. Considering the good qualitative results obtained from this pre-pilot well test, it was decided to focus on the preparation of the next phase and to pursue the pilot program in an industrial context.

Third demonstration pilot – Deep, deviated gas well (3900 mRT) - Continuous & fall-off modes

This pilot was a major step in the test qualification process. The candidate was a deep tight-gas reservoir in a heterogeneous fluvio-deltaic environment, drilled with a maximum inclination of 15 degrees and equipped with 4½" cemented tubing. The 7" casing shoe was set at 3396 m TVD and the vertical open-hole section to be tested was 473 meters thick.
The test objectives were to demonstrate the feasibility of this kind of testing method in spite of challenging wellbore conditions, while keeping costs as low as possible. Main expectations were: to prove test feasibility, to circulate at great depth a clean fluid interface in the annulus space between a production tubing and an open hole, to precisely detect the main reservoir layers seen in conventional log data, to derive a reliable permeability and skin profile through data inversion along the length of the open hole from continuous & fall-off test results (with calibration against *kh* values derived from conventional techniques) and to conduct such testing operations safely and cost-effectively.

- Several potential risks, depending upon the fluid used for the test and the operating procedures, were identified by a formal risk-assessment exercise before the pilot operations were launched. The main risk anticipated was stuck pipe, which might be caused by differential sticking across depleted zones or by mechanical instability of the coal layers frequently encountered while drilling this type of reservoir. A dedicated trip with a work string would have added exposure time and increased the stuck pipe risk, especially if the bottom hole assembly (BHA) incorporated large-OD subs such as gauge carriers. This risk was not considered acceptable. Moreover, if a work string was lowered down the well, the tubing would be continuously rotated in order to mitigate sticking potential along the open hole. This rotation would imply no wellhead pressure on the annulus side, seriously complicating test interpretation. Drill-pipe plugging, in the event of open-hole destabilization by brine, was also seen as a possible severe risk associated with reverse circulation, the procedure followed during the first test. More specifically, reverse circulation scenarios could lead to very severe situations if circulation was lost for any reason (DP plugged or pack-off in the annulus) as no float valve or check valve can be used in such cases.
- Lastly, the specific gravities of the two liquids must be such that well pressure will be greater than reservoir pressure at all times in order to keep circulating procedures as simple as possible, without the requirement to apply back pressure at the surface. At these depths, a 0.1 difference in specific gravity between fluids is more than sufficient (resulting in a 40-bar pressure difference at 4000-m TVD. In our case, standard $CaCl_2$ brine with a specific gravity of 1.35 was used as the specific gravity of the mud in the last drilling phase was about 1.25. In the event of a higher reservoir pressure, the use of complex brine would have been necessary, leading to higher costs and trickier fluid handling.

The solution selected to minimize the risks identified above was to conduct the test through the production tubing once the tubing hanger had been landed and locked in the wellhead. A direct circulation of the heavier brine was implemented, resulting in wellbore pressures greater than reservoir pressure at all times without needing to choke returns. The main lines of the sequence were as follows: run production tubing with float equipment as for a normal completion, land and lock hanger, perform the well test in direct circulation and pump cement job. The drawbacks of this option were that: no downhole pressure data acquisition was possible; displacement of a viscous fluid (drilling mud) by a less viscous fluid (brine) was not ideal for maintaining good interface quality while pumping down in the tubing, which might have led to poor-quality results; furthermore, direct circulation entailed a full circulation cycle when the test sequence across the open hole was repeated for the second phase of the test, based on steps and fall-offs. However, running a pilot test in its industrial configuration offered substantial advantages for the visibility of this new technique, considering that:

- In principle, a test like this does not require downhole pressure measurements. Depth matching of continuous test data against conventional static log data accounts for fluid density variation, downhole conditions and pressures losses during the test. However, in a pilot phase for new fields, downhole gauges would be invaluable for calibrating subsequent well test acquisitions more accurately.
- Standard completion procedures incorporate a calibration plug pumped before the cement job in order to accurately measure the displacement volume behind the cement job. The calibration plug includes a

burst disc with a differential pressure commonly set at 2000-2500 psi to clearly detect when the plug reaches the float collar. For the test, a specific calibration plug rated at 100 psi, to prevent a strong surge of the brine through the mud upon bursting, was used to provide a solid interface between drilling mud and brine while displacing down the tubing.

- The measurements in this case took about 30 hours' rig time for the two test sequences (continuous & fall-off phase), including rig-up of surface lines and data acquisition equipment. The recording time for 500 meters of open hole in the continuous phase was 4 hours, i.e. interface speed about 2 meters/min. Sensitivity to circulation rate will be analyzed to define the optimum pumping rate while logging. A circulation rate of up to 4 meters/min, i.e. about 2 hours for 500 meters' logging, was tested in a repeat section, showing similar events. Furthermore, fall-off tests recorded in a second test would not always be necessary. Optimized testing procedures to further reduce test duration to a few hours are currently being considered.

All the measurements (pressure & flow metering) were properly performed with no data loss. Outcomes from the pre-pilot shallow well, which had been run with the same test configuration and the same measurement devices, were critical for the success of this new pilot operation. The well test layout (**Figure 8)** enabled all the data needed to be properly recorded and a very precise fluid displacement was achieved thanks to the calibration plug (**Picture 1)** separating brine from drilling mud while pumping down the central production tubing. With the help of a pressure regulator **(Picture 2),** efficient constant wellhead pressure could be maintained too**.** No operational problems were encountered during the test phase and no pack-offs generated by destabilization from shale or coal layers were experienced during the circulation phases. The operational side of the test was considered as a success at this stage, as a clear data set was obtained in the challenging conditions of this pilot. The two main issues, pointed out at the beginning of the project, needed however to be addressed: the ability of the mud cake to allow brine injection into the formation and the possibility of precisely locating well test events along the borehole.

- Brine was injected into the formation during the continuous phase. This confirms preliminary laboratory experiments carried out to check whether viscous brine could penetrate into the formation in presence of an efficient mud filter cake. Filtration rates of 1.35 sg $CaCl_2$ brine through aloxite discs with permeabilities similar to those of the formations were tested in the laboratory. The discs were initially subjected to prolonged exposure to a representative OBM used when drilling similar wells, allowing a filter cake to build up. This was an attempt to recreate the situation that would be encountered on the pilot well when $CaCl_2$ brine is introduced into a well that had been drilled with OBM. One positive outcome from the laboratory study was that the filtration rates of low-viscosity brines are governed rapidly by the permeability of the aloxite discs: the greater the permeability, the faster the filtration of the brine through the disc. The effect of the differential pressure applied to the aloxite disc is marginal. Here, with no viscosity effects, the only limit to filtration is the relative permeability of the discs. For the high-permeability discs, this limit is exceeded almost immediately whereas for the lower permeability discs, the rate of filtration throughout the test is restricted **(Figure 9).** These results show that a mud filter cake would not act as an efficient barrier in presence of low-viscosity brine and that brine filtration would directly depend on formation permeability.
- **Figure 10** shows the raw data of the lower section of the continuous test phase without any depth matching. The differential flow rate between brine at the inlet flow meter and mud at the outlet flow meter versus depth and its derivative to depth are simply displayed in the last two tracks of the log. Other conventional logs (Gamma Ray, lithology, Nphi & Rhob, Resistivity and total Gas) are shown in the first tracks of the display. Contrasted responses at each change of lithology, similar to those observed in the second pilot (**Figure 7**), can been seen. Even in the harsh environment of this deep deviated well, the injectivity indicator seems to concur closely with log events (highlighted in green). Detailed analysis of the log, for example between 3610-3620 mRT for the deepest reservoir, indicated that injectivity increases in the reservoir layer. Moreover, the porosity reduction in the middle of the reservoir can be perfectly seen from the well test data and the differential flow rate signature is, surprisingly very similar to the total gas measured while drilling. Other similar signatures with total gas can be seen also above. Some coal layers can also react sharply to the brine injection (at 3750 mRT), while others, as at 3840 mRT, do not seem to react. Some indications of permeation in the log (highlighted in red) do not seem to be correlated with log responses on particular levels, which may indicate other events not seen in conventional logs. The test results show that variation of the brine injectivity across layers is very sharp, indicating a more dynamic variation, such as a permeability variation in a reservoir, than in static logs. The raw test results demonstrate that it is possible to obtain a clean fluid interface while circulating at great depth and to achieve precise location of injectivity events. This suggests also that the open hole was very regular, as expected while drilling with oil-based mud, as depth matching was not necessary.

Many interpretations are necessary to go a step further than a qualitative tool and to qualify the method against conventional *kh* data. In particular, it must be demonstrated that the test provides access to the *kh* of the undamaged zone. As soon as it is available, the test interpretation will be meticulously compared to conventional data.

Ongoing action focuses on the interpretation model, to represent the sharp variation of differential flow at the layer interfaces. **Figure 11** shows a simulation of the injection profile when the brine/mud interface is rising along the borehole. The steep variations in the injection brine flow rate at the interfaces are related to the permeability contrasts, as seen in **Figure 12** from simulation and very well in the field during the second pilot, as shown in **Figure 7**. The brine injectivity trend decreased slightly in the less permeable part of the reservoir but dropped steeply when the fluid interface reached the overlying shale layer.

This phenomenon is favorable to test monitoring, as the injection flow rate should remain fairly low to avoid stopping the test and switching to the rig pumps in case of massive brine injection in the formation leading to a strong decrease of the wellhead flowing pressure. Small pumps may therefore be used with slight variation in delivery rate in the course of the test. This also seems favorable to the inversion process as the first layers encountered during the rise of the fluid interface would not be very important for the behavior of the subsequent overlying layers. The robustness of the inversion process must nevertheless be demonstrated by comparing results from the inversion against *kh* values derived from conventional techniques (core, MDT, well test) and this will be the priority of the ongoing work to qualify the new well test method.

Conclusions

1. A new well test for tight-gas reservoirs, adapted from techniques used in the salt cavern industry, is proposed. The core idea of the technique is to create a clean fluid interface separating two fluids with contrasting densities and viscosities in order to differentiate fluid leak-off rates in two different parts of the open hole. By circulating this interface in the well, the differential flow rate between the two fluids versus depth returns an estimation of a continuous injectivity profile along the open hole. Lastly, this new method aims to derive continuous *kh* and skin profiles but still needs to be qualified against conventional *kh* data. In particular, it must be demonstrated that the test offers access to the *kh* of the undamaged zone of the wellbore.
2. To date, three well tests have been carried out in various types of wells showing good correlations with conventional logs. To go a step further than a qualitative tool, a deconvolution of the time-dependent and interface-depth-dependent permeation flows is necessary. An inversion process accounting for the injection history in the various layers is being developed with the objective of deriving a continuous *kh* and skin profile.
3. To minimize operational risks, the test is conducted through the production tubing once the tubing hanger has been landed in the wellhead. Direct circulation of a heavier fluid also mitigates operational risks as it allows simple circulating procedures. Two acquisition modes are possible: a continuous mode where a brine/mud interface is displaced along the borehole by pumping brine in the tubing at a constant pressure and circulating out mud from the annulus; a stationary mode where the entire wellbore is pressurized with the interface at different depth intervals and fall-offs resulting from fluid seepage to the rock formation are interpreted successively. Optimized testing procedures to further reduce the test duration to a few hours are being considered.
4. This method can be tuned to all type of reservoirs: Tight-Gas Reservoirs, Gas Shale, overburden layers and conventional reservoirs by adapting the liquid viscosities to the average permeability of the tested interval.

Acknowledgements

The authors thank Total management for permission to publish the results of this research work. They also wish to thank Vincent de Greef & Jean-François Béraud from the *Ecole Polytechnique* (France) for their extensive contribution and dedication during the various pilot-test operations.

Nomenclature

β_1	Compressibility factor of light liquid	$\times 10^{-5}$ /bar
β_2	Compressibility factor of heavy liquid	$\times 10^{-5}$ /bar
β_{ann}^{ext}	Compressibility factor of outer annulus	$\times 10^{-5}$ /bar
β_{ann}^{int}	Compressibility factor of inner annulus	$\times 10^{-5}$ /bar

β_d	Compressibility factor of outer borehole	$\times 10^{-5}$ /bar
β_d^{int}	Compressibility factor of inner borehole	$\times 10^{-5}$ /bar
β_{tub}^{int}	Compressibility factor of inner tubing	$\times 10^{-5}$ /bar
β_{tub}^{ext}	Compressibility factor of outer tubing	$\times 10^{-5}$ /bar
βV	Well compressibility	liters/bar
D_{tub}^{int}	Inside diameter of the tubing	mm
D_{tub}^{ext}	Outside diameter of the tubing	mm
E_{tub}	Young's modulus of tubing steel	MPa
E_R^d	Young's modulus of borehole	MPa
e_{tub}	Thickness of the tubing	mm
H_{cas}	Casing shoe depth	m
H_d	Borehole height	m
h	Interface location from bottom	m
λ	Casing/cement compressibility factor	—
ν_R^d	Poisson's ratio of borehole	—
ν_{tub}	Poisson's ratio of tubing steel	—
Q_1	Light liquid permeation flow	liters/min
Q_{ann}^{wh}	Light liquid circulation flow rate	liters/min
Q_2	Heavy liquid permeation flow	liters/min
Q_{tub}^{wh}	Heavy liquid circulation flow rate	liters/min
r_{tub}^{ext}	Tubing outer radius	mm
ρ_1	Light liquid density	kg/m^3
ρ_2	Heavy liquid density	kg/m^3
S_{ann}	Annulus cross-section (cemented part)	liters/m
S_{tub}	Tubing cross-section	liters/m
$\tau_{tub} = D_{tub}^{\text{int}} / D_{tub}^{ext}$	Reduced radius of the tubing	—
Σ	Borehole annulus cross-section	liters/m
V_{ann}	Annulus volume	m^3
V_{tub}	Tubing inner volume	m^3
z	Depth	m
z_i	Interface depth	m

References

Holditch S.,"*Tight Gas Sand"*, SPE 103356.

Brouard B., Bérest P. and Durup J.G. *In-situ salt permeability testing.* In Proc. S.M.R.I. Fall Meeting, Albuquerque, USA, pages 139-157, 2001.

Alpak F.O., Torres-Verdi C. and Sepehrnoori K. (2004) *Estimation of axisymmetric spatial distributions of permeability and porosity from pressure-transient data acquired with in situ permanent sensors.* Journal of Petroleum Science and Engineering, 44, pp. 231-267.

Luersen M.A. and Le Riche R. (2004) *Globalized Nelder-Mead method for engineering optimization*. Computers and Structures, 82, pp. 2251-2260.

Rahman M.A and Mattar L. (2007) *New analytical solution to pressure transient problems in commingled, layered zones with unequal initial pressures subject to step changes in production rates.* Journal of Petroleum Science and Engineering, 56, pp. 283-295.

Bérest P., Brouard B., Bergues J., Frelat J. and Durup J.G. Salt caverns and the compressibility factor. In Proc. S.M.R.I. Fall Meeting, El Paso, USA, pages 29-48, 1997.

Brouard B., Bérest P., Caligaris C., Frangi A., Hévin G. and Pichery T. *Numerical Computations of the Mechanical Behaviour of Cemented Casings Submitted to Large and Fast Pressure Variations*. In Proc. S.M.R.I. Fall Meeting, Rapid City, USA, pages 217-232, 2006.

SI Metric Conversion Factors

psi × 6.894 757 E+00 = kPa

* Conversion factor is exact.

Appendix

The flow rates injected in the formation (Q_1 and Q_2), the pumped and withdrawn flow rates at the wellhead (Q_2^{wh} and Q_1^{wh}), the interface displacement rate ($\dot{h}$) are related to the wellhead pressure evolution rates through the mass-balance and equilibrium conditions:

$$\begin{bmatrix} Q_1 + Q_{ann}^{wh} \\ Q_2 - Q_{tub}^{wh} \\ (\rho_2 - \rho_1) g\dot{h} \end{bmatrix} = [M] \begin{bmatrix} \dot{P}_{tub}^{wh} \\ \dot{P}_{ann}^{wh} \end{bmatrix} = \begin{bmatrix} C & -D \\ -E & F \\ A & -B \end{bmatrix} \begin{bmatrix} \dot{P}_{tub}^{wh} \\ \dot{P}_{ann}^{wh} \end{bmatrix}$$

Where

$$\begin{cases} A = 1 + \beta_2 g \rho_2 \left(H_{cas} + H_d - h \right) \\ B = 1 + \beta_1 g \rho_1 \left(H_{cas} + H_d - h \right) \\ C = \dfrac{\Sigma A}{(\rho_2 - \rho_1) g} + V_{ann} \beta_{\text{ann}}^{ext} + \Sigma \left(H_d - h \right) \beta_{\text{d}}^{ext} \\ D = \dfrac{\Sigma B}{(\rho_2 - \rho_1) g} + V_{ann} \left(\beta_1 + \beta_{ann}^{\text{int}} \right) + \Sigma \left(H_d - h \right) \left(\beta_1 + \beta_d^{\text{int}} \right) \\ E = \dfrac{\Sigma A}{(\rho_2 - \rho_1) g} + V_{tub} \left(\beta_2 + \beta_{tub}^{\text{int}} \right) + \Sigma h \left(\beta_2 + \beta_d \right) \\ F = \dfrac{\Sigma B}{(\rho_2 - \rho_1) g} + V_{tub} \beta_{tub}^{ext} \end{cases}$$

$$\begin{cases} \beta_{ann}^{\text{int}} = \dfrac{2\pi}{S_{ann}} \left[\hat{\lambda} \left(r_{ann}^{\text{int}} \right)^2 + \dfrac{(1 + \nu_{tub}) \left(r_{tub}^{ext} \right)^2}{E_{tub}} \dfrac{\left[\tau_{tub}^2 - (1 - 2\nu_{tub}) \right]}{\left(1 - \tau_{tub}^2 \right)} \right] \\ \beta_{ann}^{ext} = \dfrac{4\pi \left(1 - \nu_{tub}^2 \right) \left(r_{tub}^{ext} \right)^2 \tau_{tub}^2}{S_{ann} E_{tub} \left(1 - \tau_{tub}^2 \right)} \\ \beta_{tub}^{\text{int}} = \dfrac{2(1 + \nu_{tub})}{E_{tub} \left(1 - \tau_{tub}^{\ 2} \right)} \left[1 + (1 - 2\nu_{tub}) \tau_{tub}^{\ 2} \right] \\ \beta_{tub}^{ext} = \dfrac{4\left(1 - \nu_{tub}^{\ 2} \right)}{E_{tub}} \\ \beta_d = \dfrac{2\left(1 + \nu_R^d \right)}{E_R^d} \\ \beta_d^{\text{int}} = \dfrac{\pi}{\Sigma} \left[\dfrac{\left(1 + \nu_R^d \right) \left(r_d \right)^2}{2E_R^d} + \dfrac{2(1 + \nu_{tub}) \left(r_{tub}^{ext} \right)^2}{E_{tub}} \dfrac{\left[\tau_{tub}^2 - (1 - 2\nu_{tub}) \right]}{\left(1 - \tau_{tub}^2 \right)} \right] \\ \beta_d^{ext} = \dfrac{4\pi \left(1 - \nu_{tub}^2 \right) \left(r_{tub}^{ext} \right)^2 \tau_{tub}^2}{\Sigma E_{tub} \left(1 - \tau_{tub}^2 \right)} \end{cases}$$

Figures

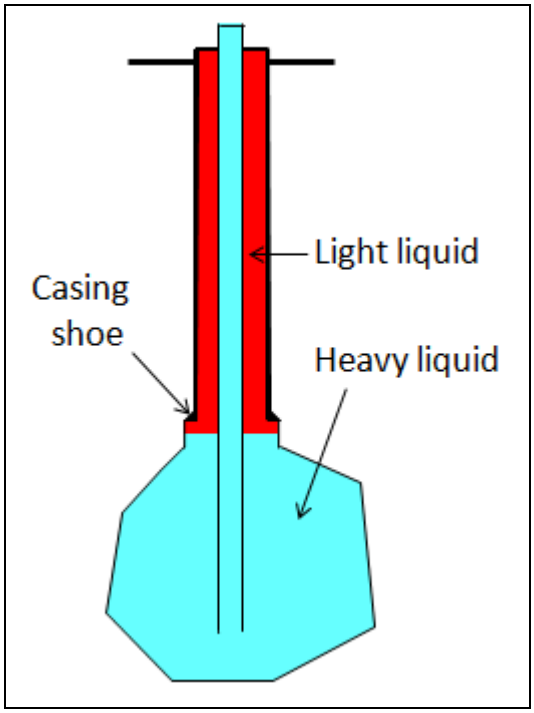

Figure 1 – Tightness test in the context of solution-mined caverns

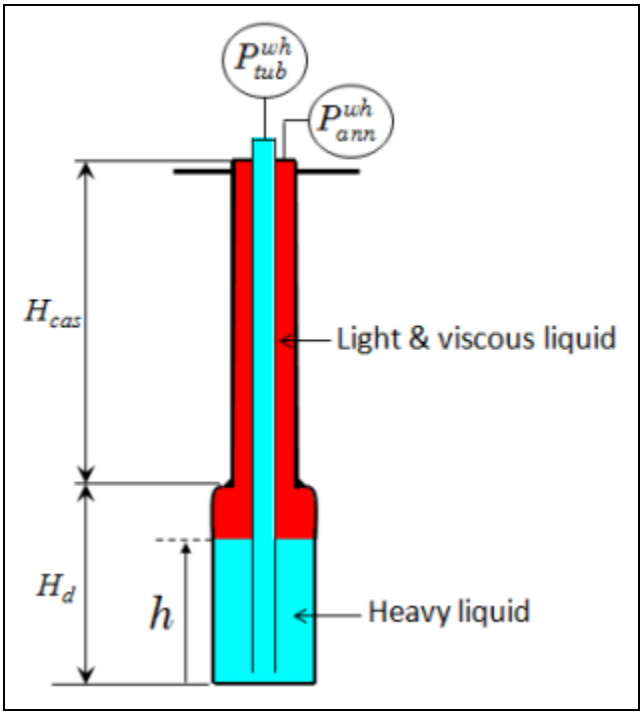

Figure 2 – Well test Log configuration

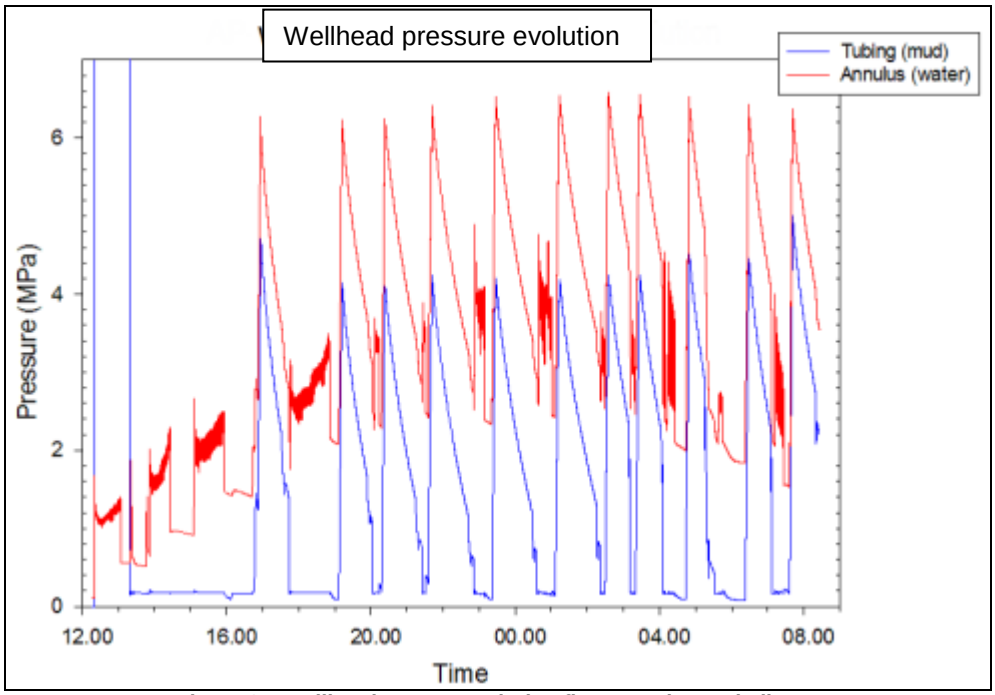

Figure 3 – Wellhead pressures during first experimental pilot

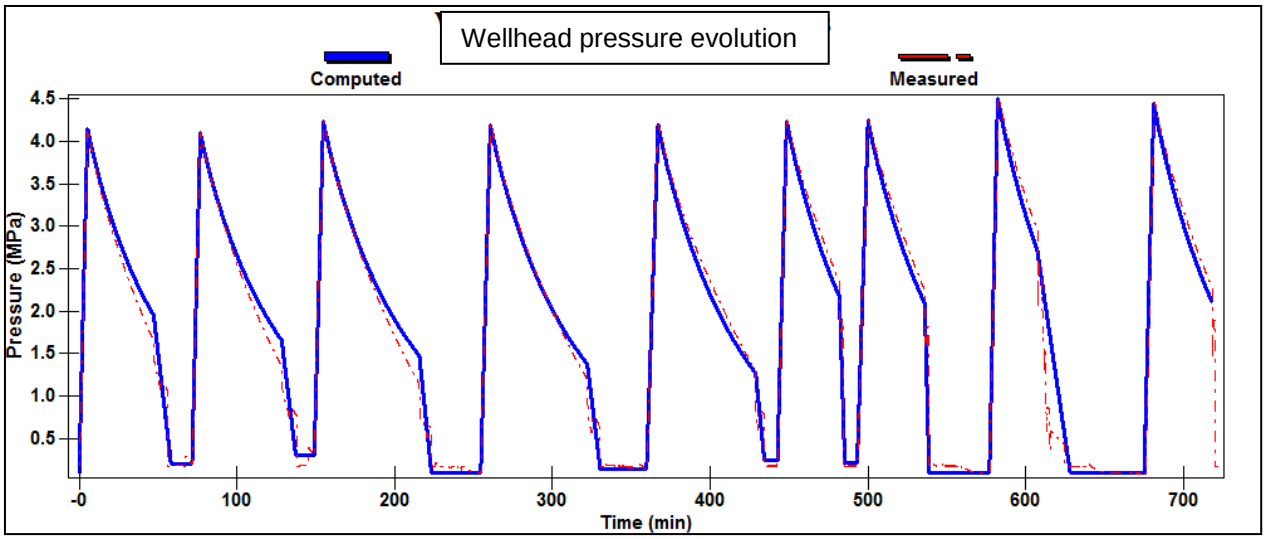

Figure 4 – History matching of tubing wellhead pressure for first experimental pilot

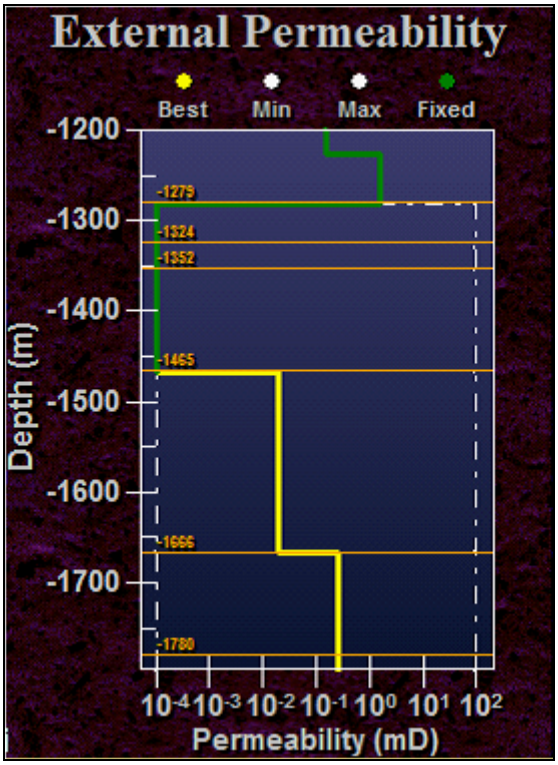

Figure 5 – Back-calculated estimated permeability profile from first experimental pilot

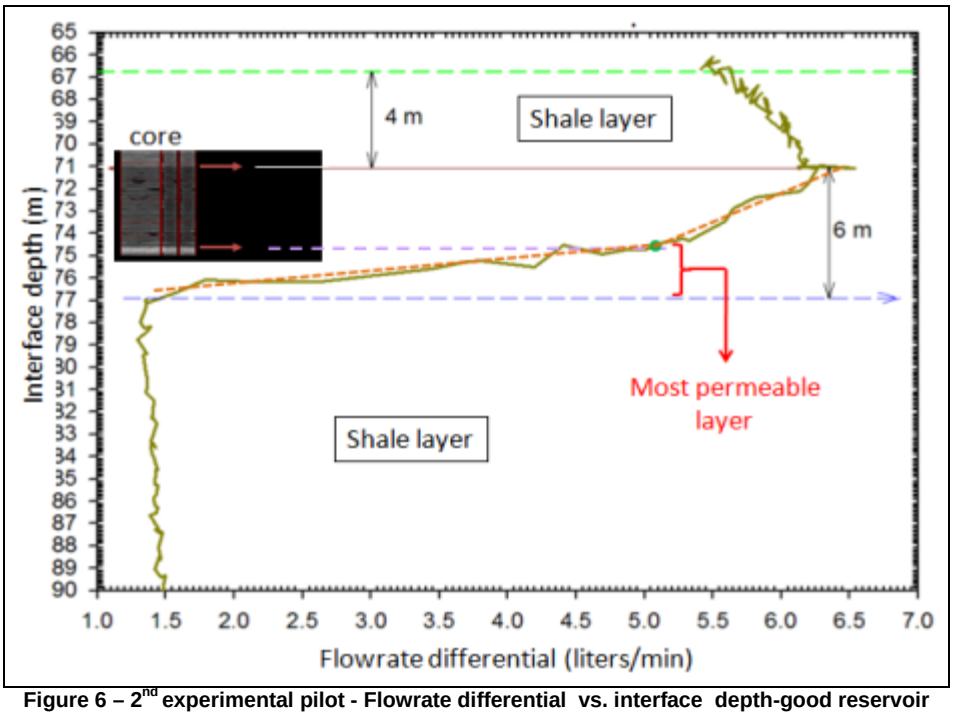

Figure 6 – 2nd experimental pilot - Flowrate differential vs. interface depth-good reservoir (top of the open-hole section).

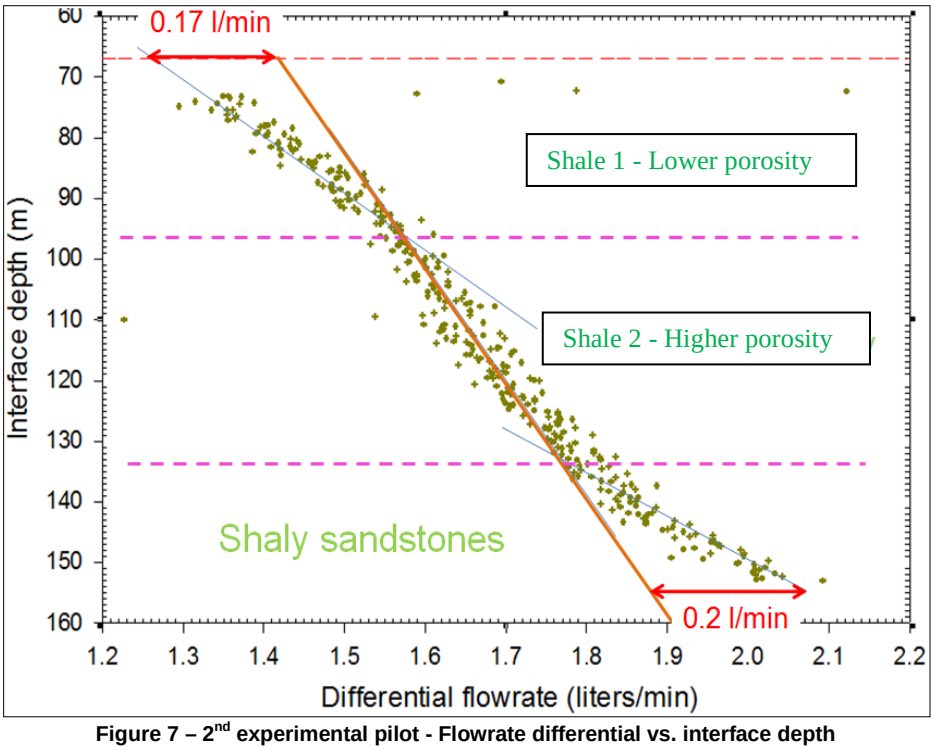

Figure 7 – 2nd experimental pilot - Flowrate differential vs. interface depth (bottom of the open-hole section)

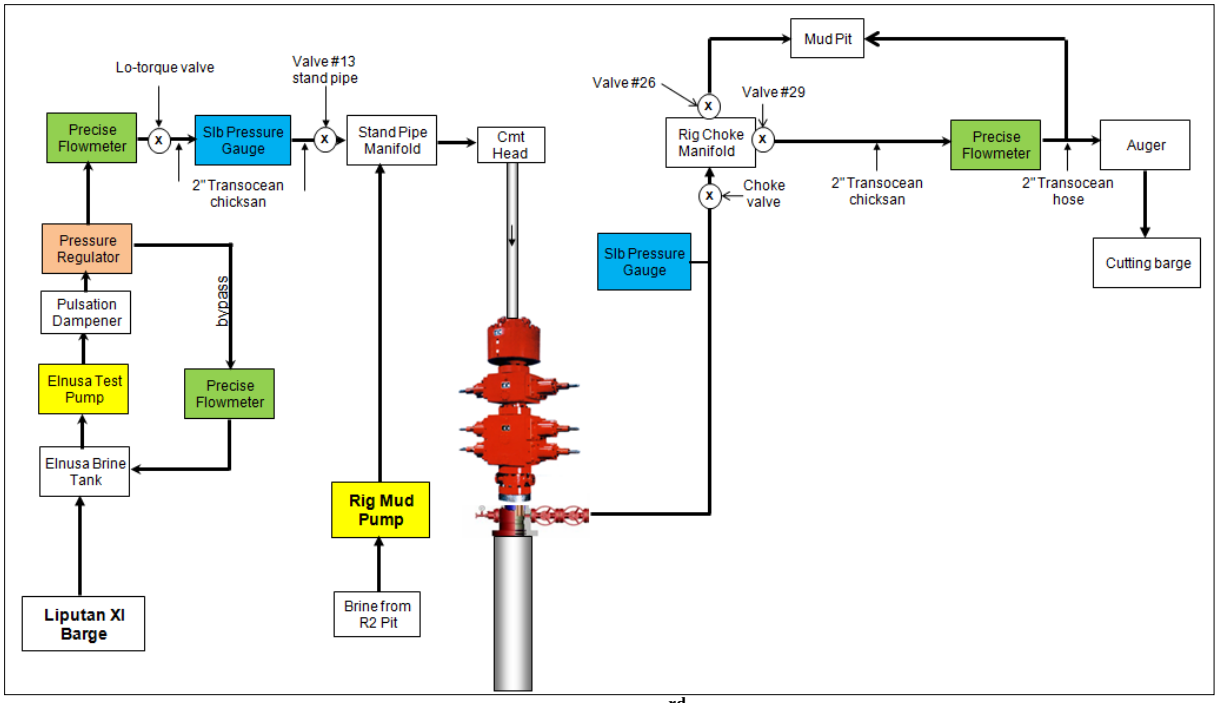

Figure 8 – Well test Pilot layout - 3rd demonstration pilot

Picture 1 – Calibration plug.

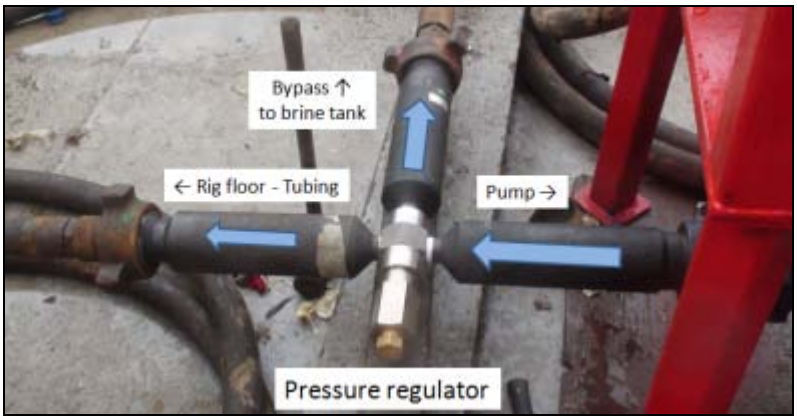

Picture 2 – Pressure regulator used during the 3rd demonstration pilot

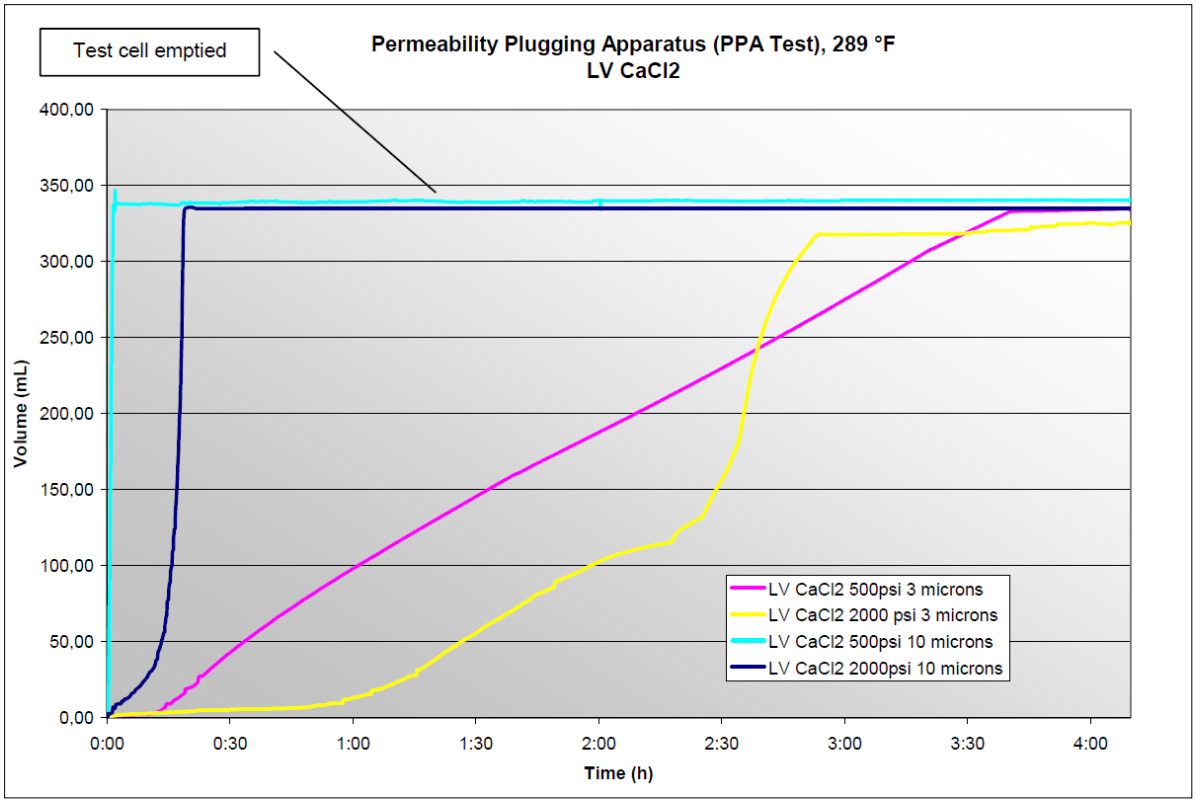

Figure 9 – Laboratory test showing brine filtration across mud cake for various aloxite disc sizes

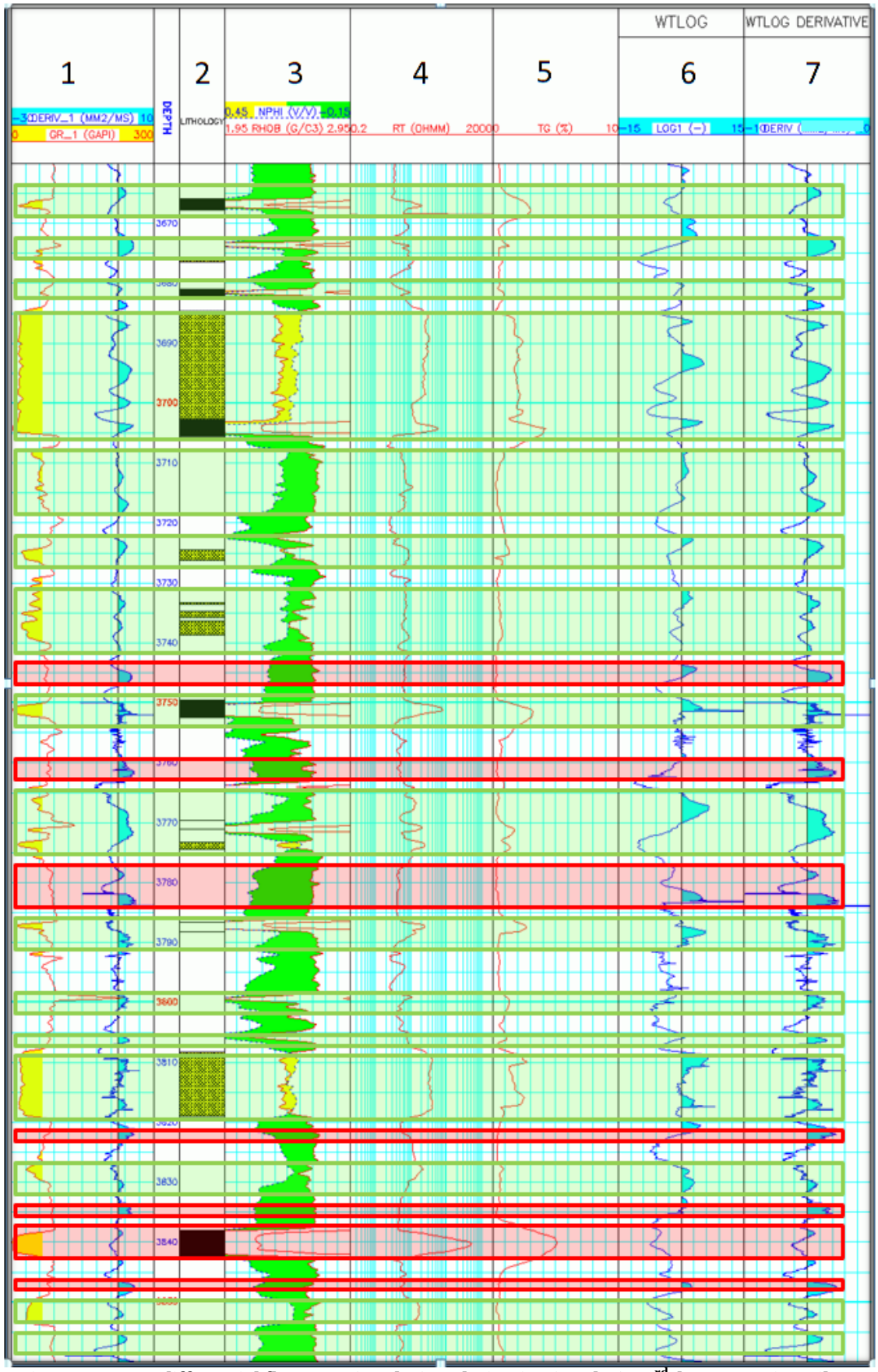

Figure 10: Raw differential flowrates (track 6) & derivative (track 7) - 3rd demonstration pilot

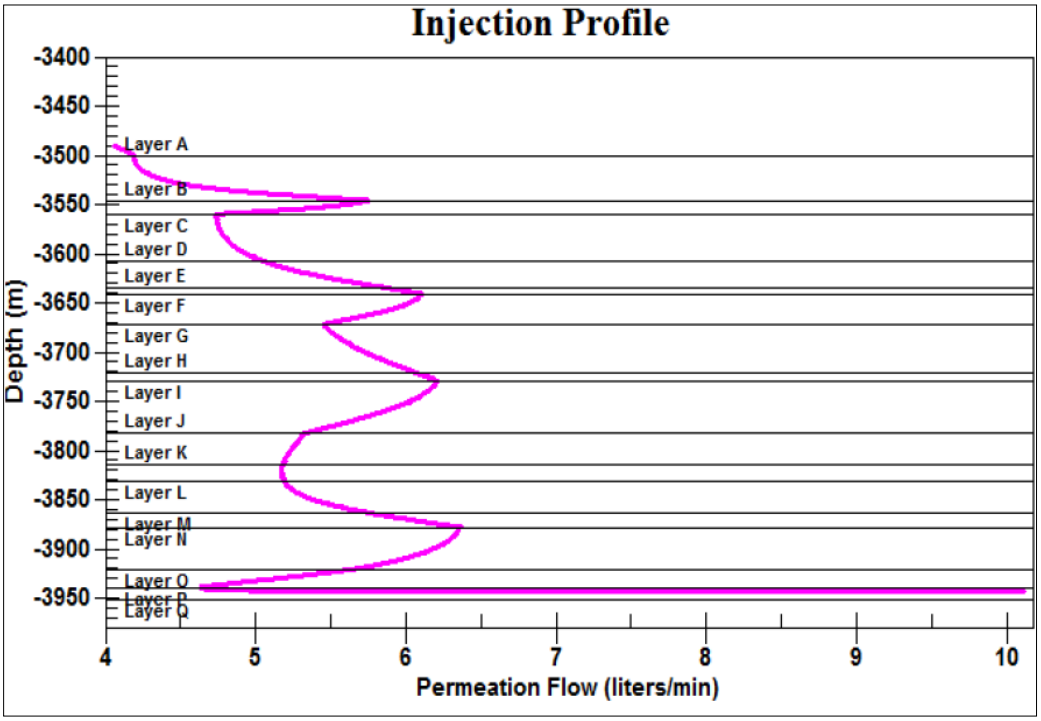

Figure 11: Well test design example from simulation.

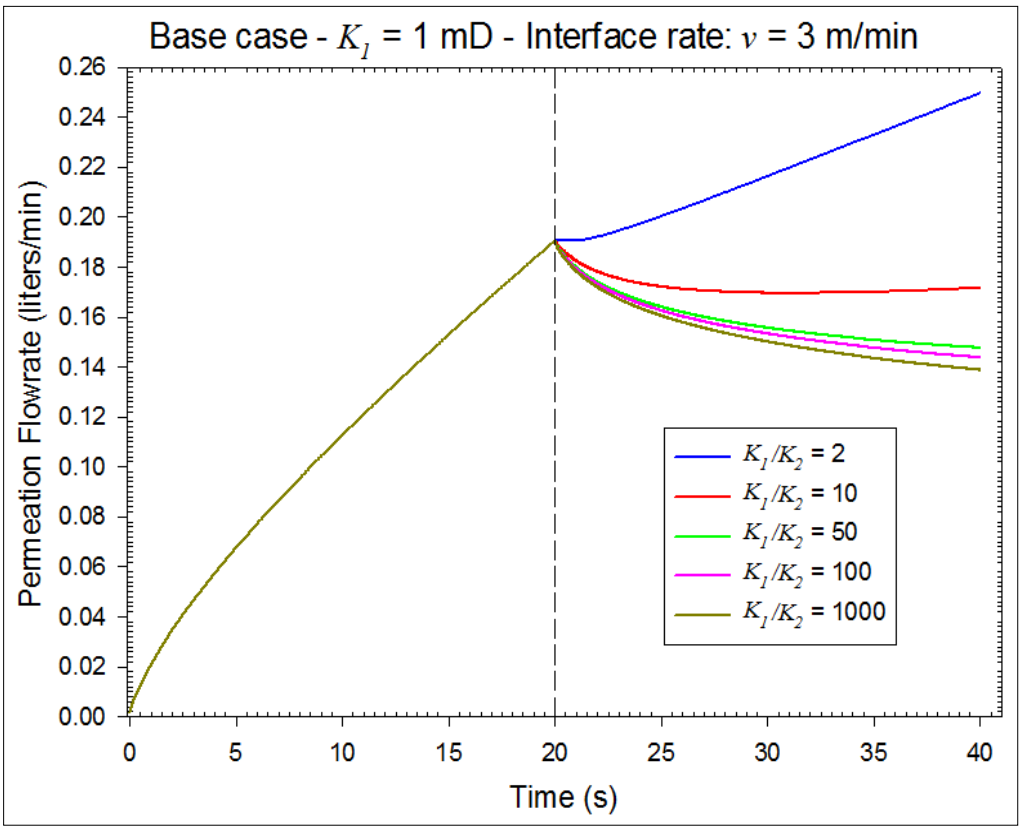

Figure 12: Permeation flow vs. time as a function of layer permeability contrast